



UNIVERSITY
OF WOLLONGONG
AUSTRALIA

University of Wollongong
Research Online

Faculty of Science, Medicine and Health - Papers:
Part B

Faculty of Science, Medicine and Health

2018

The ANSTO - University of Wollongong in-situ ^{14}C extraction laboratory

Reka H. Fulop

University of Wollongong, rfulop@uow.edu.au

David Fink

ANSTO, dfink@uow.edu.au

Bin Yang

ANSTO, Harbin Institute of Technology

Alexandru Tiberiu Codilean

University of Wollongong, codilean@uow.edu.au

A.M. Smith

ANSTO

See next page for additional authors

Publication Details

Fulop, R., Fink, D., Yang, B., Codilean, A. T., Smith, A., Wacker, L., Levchenko, V. & Dunai, T. J. (2018). The ANSTO - University of Wollongong in-situ ^{14}C extraction laboratory. *Nuclear Instruments and Methods in Physics Research Section B: Beam Interactions with Materials and Atoms*, Online First 1-7.

Research Online is the open access institutional repository for the University of Wollongong. For further information contact the UOW Library:
research-pubs@uow.edu.au

The ANSTO - University of Wollongong in-situ ^{14}C extraction laboratory

Abstract

We present our first ^{14}C in-situ results for calibration and system blanks from the recently completed Australian Nuclear Science and Technology Organisation (ANSTO) - University of Wollongong (UOW) in-situ ^{14}C extraction system. System performance parameters and quality is evidenced by low ^{14}C blanks and good reproducibility for multiple targets from different reference materials. The ^{14}C extraction scheme exploits the high temperature phase transformation of quartz to cristobalite in order to quantitatively extract the carbon as CO_2 . The in-situ ^{14}C extraction system comprises three independently operated and modular units that are used for initial in-vacuo removal of meteoric ^{14}C , followed by offline high-temperature heating of quartz to release trapped cosmogenic in-situ ^{14}C , and finally CO_2 gas purification and mass measurement. The design allows for rapid sample throughput of about 6 samples per week with samples masses ranging between 0.5 and 4 g of clean quartz. Other features include single-pass catalytic oxidation using mixed copper (I,II) oxide as catalyst, use of UHV-compatible components and of vacuum annealed copper tubing. We present results for sets of purified quartz samples prepared from CRONUS-A, CRONUS-R and CRONUS-N inter-comparison materials, with final averages consistent with published values. Following extraction and cleaning, CO_2 gas aliquots for some of the samples were analysed using the ETH Zürich CO_2 gas ion source at the ETH MICADAS AMS facility in addition to CO_2 being graphitised using the ANSTO laser-heated graphitisation micro-furnace and then analysed on ANSTO's ANTARES AMS facility. System blanks using either CO_2 or graphite ion-sources at both facilities are on the order of $\sim 1 \times 10^4$ atoms.

Publication Details

Fulop, R., Fink, D., Yang, B., Codilean, A. T., Smith, A., Wacker, L., Levchenko, V. & Dunai, T. J. (2018). The ANSTO - University of Wollongong in-situ ^{14}C extraction laboratory. Nuclear Instruments and Methods in Physics Research Section B: Beam Interactions with Materials and Atoms, Online First 1-7.

Authors

Reka H. Fulop, David Fink, Bin Yang, Alexandru Tiberiu Codilean, A M. Smith, Lukas Wacker, Vladimir Levchenko, and Tibor J. Dunai

1 The ANSTO – University of Wollongong *in-situ* ¹⁴C extraction laboratory

2
3 Réka-H. FÜLÖP (1,2), David FINK (2), Bin YANG (2), Alexandru T. CODILEAN (1), Andrew SMITH (2),
4 Lukas WACKER (3), Vladimir LEVCHENKO (2), and Tibor J. DUNAI (4).

5
6 (1) School of Earth and Environmental Sciences, University of Wollongong, 2522, Wollongong, Australia

7 (2) Australian Nuclear Science and Technology Organisation (ANSTO), Lucas Heights NSW 2234, Australia

8 (3) Ion Beam Physics, ETH Zürich, 8093 Zürich, Switzerland

9 (4) Institute of Geology and Mineralogy, University of Cologne, 50674 Cologne, Germany

10
11 *Corresponding author:* R-H. Fülöp, rfulop@uow.edu.au

12 13 **Abstract**

14 We present our first ¹⁴C *in-situ* results for calibration and system blanks from the recently completed
15 Australian Nuclear Science and Technology Organisation (ANSTO) - University of Wollongong (UOW) *in-*
16 *situ* ¹⁴C extraction system. System performance parameters and quality is evidenced by low ¹⁴C
17 blanks and good reproducibility for multiple targets from different reference materials. The ¹⁴C
18 extraction scheme exploits the high temperature phase transformation of quartz to cristobalite in
19 order to quantitatively extract the carbon as CO₂. The *in-situ* ¹⁴C extraction system comprises three
20 independently operated and modular units that are used for initial *in-vacuo* removal of meteoric ¹⁴C,
21 followed by offline high-temperature heating of quartz to release trapped cosmogenic *in-situ* ¹⁴C and
22 finally CO₂ gas purification and mass measurement. The design allows for rapid sample throughput of
23 about 6 samples per week with samples masses ranging between 0.5 to 4 grams of clean quartz.
24 Other features include single-pass catalytic oxidation using mixed copper (I,II) oxide as catalyst, use
25 of UHV-compatible components and of vacuum annealed copper tubing. We present results for sets
26 of purified quartz samples prepared from CRONUS-A, CRONUS-R and CRONUS-N inter-comparison
27 materials, with final averages consistent with published values. Following extraction and cleaning,
28 CO₂ gas aliquots for some of the samples were analysed using the ETH Zürich CO₂ gas ion source at
29 the ETH MICADAS AMS facility in addition to CO₂ being graphitised using the ANSTO laser-heated
30 graphitisation micro-furnace and then analysed on ANSTO's ANTARES AMS facility. System blanks
31 using either CO₂ or graphite ion-sources at both facilities are on the order of $\sim 1 \times 10^4$ atoms.

32
33 **Keywords:** *In-situ* ¹⁴C; Cosmogenic nuclide; ¹⁴C extraction scheme.

34 35 **1. Introduction**

36 Due to its very short half-life (5730 years) compared to that of ^{10}Be ($\sim 1.4\text{Ma}$), *in-situ* ^{14}C is
37 substantially more sensitive to short-term variations in geological process rates. Often, it is the case
38 that the erosion of steep mountains via stochastic mass wasting processes, and the dynamics of
39 sediment transport, storage, and recycling, may occur over timescales that are too short to be
40 detected by the more well established cosmogenic nuclides, namely ^{10}Be and ^{26}Al . *In-situ* ^{14}C is then
41 ideally suited for such short term and transient processes. For example, when used in combination
42 with ^{10}Be and ^{26}Al , rapid fluctuations in process rates and/or identification of recent sediment
43 recycling and transfer can be measured accurately (e.g., Hippe et al., 2012; Kober et al., 2012).
44 Cosmogenic radionuclide exposure dating of glacial landforms has made an exceptionally large
45 contribution to glacial chronology studies (Balco et al., 2011). For example, ^{10}Be and ^{26}Al have been
46 used to reconstruct Antarctica's ice volume changes over the past 4 Ma – with emphasis on post Last
47 Glacial Maximum (LGM) ice volume contributions to global sea level changes –, and to determine the
48 degree of synchronicity of inter-hemispheric mid-latitude glacial retreat. Despite these advances,
49 many assumptions are used in converting measured ^{10}Be concentrations to 'true' exposure ages.
50 When coupled with a ^{10}Be exposure age of a glacially transported erratic boulder, *in-situ* ^{14}C can
51 provide a unique way to validate that the measured ^{10}Be concentration in such glacial deposits
52 reflect a true exposure age void of inheritance. Holocene and late Pleistocene glacial exposure ages
53 from polar regions are especially prone to misinterpretation due to variable inheritance. Currently,
54 all Antarctic and Greenland glacial studies attempting to 'map' polar LGM extent may carry within
55 their sample population erroneous ^{10}Be ages. All of the above makes *in-situ* ^{14}C an important addition
56 to the cosmogenic radionuclide toolkit.

57

58 Despite the obvious need for *in-situ* ^{14}C in the Earth sciences, the routine analysis of this radionuclide
59 is only now reaching the end of a very protracted development phase (Lifton et al., 2001; Hippe et
60 al., 2009; Fülöp et al., 2010; Goehring et al., 2014; Fülöp et al., 2015a). The major obstacle revolved
61 around being able to quantitatively, reliably, and economically extract from a few grams of purified
62 quartz the small amounts of *in-situ* ^{14}C produced in terrestrial samples, while at the same time also
63 removing the more abundant 'meteoric' ^{14}C produced in the atmosphere (Lal and Jull, 1994). Due to
64 it being tightly bound in the silicate matrix, the extraction of *in-situ* ^{14}C is rarely possible without the
65 fusion of the silicate minerals (Des Marais, 1983; Brown et al., 1984). The diffusion of CO_2 through
66 the crystal lattice (Cresswell et al., 1983) in silicate melts is largely independent of composition
67 (Watson et al., 1982), and trapped *in-situ* ^{14}C is released from the host mineral at temperatures
68 exceeding $1000\text{ }^\circ\text{C}$. Studies in meteorites have suggested a grain-size dependence; carbon being
69 released from finely powdered samples at lower temperatures, namely $700\text{--}800\text{ }^\circ\text{C}$ (Des Marais and
70 Moore, 1984; Jull et al., 1989; Pineau and Javoy, 1994). For *in-situ* ^{14}C surface exposure dating of
71 terrestrial rocks, two different thermal extraction methods were investigated by various groups,

72 namely use of a fluxing agent to allow *in-situ* ¹⁴C release at 1100 °C (e.g., Lifton et al., 2001; Fülöp et
73 al., 2010, 2015b) and high temperature extraction at temperatures above 1500 °C (e.g., Fülöp et al.,
74 2015a; Lupker et al., 2015).

75

76 The recently completed ANSTO – UOW *in-situ* ¹⁴C extraction system was built following the design
77 developed at the University of Cologne (Fülöp et al., 2015a). This system enables fast and reliable
78 sample throughput due to a modular design and the capability of heating samples to temperatures of
79 1650 °C. Here we present results on blanks and measurements of inter-comparison materials.

80

81 **2. Extraction of *in-situ* ¹⁴C**

82 The extraction procedure of *in-situ* ¹⁴C from ultra-pure quartz aliquots consists of: (1) leaching the
83 ultra-pure quartz aliquot using HNO₃; (2) *in-vacuo* heating at 500 °C for 2 hours in fused silica tubes,
84 which are subsequently sealed (addition of a solid carbonate carrier maybe required at this step
85 when insufficient CO₂ would be released from a sample); (3) heating at 1650 °C for 2 hours in the
86 sealed fused silica tubes under a continuous flow of nitrogen gas; (4) *in-vacuo* cracking of the tubes;
87 cleaning of the released gas and quantifying the mass of CO₂; and (5) AMS measurement of either
88 CO₂ gas, or graphitised target. The current set up (Fig. 1) allows the processing of samples in batches
89 of three to six.

90

91 Steps (1) and (3) are aimed at removing meteoric ¹⁴C produced in the Earth's atmosphere,
92 transported by precipitation to the Earth's surface and incorporated into the sample. This
93 contamination is mostly removed by leaching with oxidizing acids (such as hydrofluoric acid) that are
94 commonly used during the quartz purification process (e.g., Kohl and Nishiizumi, 1992). Immediately
95 prior to the high temperature step, further pre-cleaning is essential. First the purified quartz samples
96 are leached using concentrated (69%) analytical grade HNO₃ at 120 °C and dried on a hotplate. Upon
97 drying, samples are weighed and transferred into fused silica tubes. These tubes are pre-cleaned in
98 10% analytical grade HNO₃ and heat treated at 1000 °C using a muffle furnace. After the addition of
99 sample material (and optional carbon carrier) the fused silica glass tubes are evacuated to ~10⁻⁸ mbar
100 pressure and heated to 500 °C for two hours. To permit the optional addition of a solid carbon
101 carrier, in our case CaCO₃, we limit the maximum pre-cleaning temperature to 500 °C (at higher
102 temperatures CaCO₃ starts to decompose). Following the above pre-cleaning steps, the samples are
103 free of contaminant meteoric ¹⁴C. The meteoric ¹⁴C-free samples are then sealed in their fused silica
104 glass tubes using a hydrogen and oxygen premix hand burner. In step (4) the silica tube-sealed
105 samples are heated to 1650 °C using a custom built high-temperature tube furnace with maximum
106 operating temperature of 1700 °C, under a continuous flow of nitrogen gas for two hours. The tube
107 furnace can accommodate three fused silica glass tubes to be heated simultaneously. The extraction

108 scheme exploits the phase transformation of quartz to cristobalite in order to quantitatively extract
109 the carbon as CO₂ (Fülöp et al., 2015a).

110

111 After the high-temperature heating step, the sealed silica tubes are transferred to an in-house built
112 cracking system connected to an all-metal UHV line ($\sim 10^{-8}$ mbar), with annealed copper tubing and
113 Swagelok[®] valves. The gas is led through a single-pass catalytic oxidation step. Mixed copper (I,II)
114 oxide is built into the vacuum system as catalyst and kept at 230 °C to convert all carbon species to
115 CO₂ and remove the contaminant gases (including SO_x and NO_x species) (Huang and Tsai, 2003).
116 Before and after passing through the copper oxide, the moisture released from the samples is
117 removed using two variable temperature traps. The gas is then further cleaned at -145 °C, and a
118 third variable temperature trap removes all remaining moisture. The amount of CO₂ is then
119 quantified using a heated, high-sensitivity dual-range capacitance manometer (MKS Baratron[®]).
120 Finally the purified CO₂ is sealed into a 4 mm diameter breakseal of 50 mm length using a hand torch.

121

122 Following extraction and cleaning, the CO₂ gas is converted to graphite using ANSTO's in-house built
123 laser-heated microfurnace. This setup allows for the graphitisation of microgram-sized carbon
124 samples containing between 5 and 60 µg carbon, with conversion efficiencies for 5 µg targets ranging
125 from 80% to 100% (Smith et al., 2010; Yang et al., 2015). Graphite targets are analysed using ANSTO's
126 ANTARES 10 MV tandem accelerator (Fink et al., 2004; Smith et al., 2010). To test for the effects of
127 the graphitisation process on system blanks, and to allow for comparison of results with those of
128 Fülöp et al. (2015), splits from the extracted and cleaned CO₂ gas from a selection of samples were
129 also measured using the gas ion source of the MICADAS accelerator mass spectrometer facility at
130 ETH Zürich (Fahrni et al., 2013). The MICADAS setup allows for the analysis of CO₂ samples between 3
131 and 100 µg carbon, sealed in glass tubes (Wacker et al., 2013). We calculate the final in-situ ¹⁴C
132 concentrations from the measured data as outlined in Hippe and Lifton (2014). The samples were
133 measured in 2016 and 2017, and we use a mean lifetime of 8223 years in calculations.

134

135 **3. Results and Discussion**

136

137 **3.1. Instrumental setup**

138 The ANSTO – UOW *in-situ* ¹⁴C extraction system is based on the design developed at the University of
139 Cologne and described in Fülöp et al. (2015a). Although small modifications were made to several
140 components, the same modular design, consisting of three independent components, was
141 maintained (Fig. 1). The modular design presents several advantages over other existing designs.
142 First, each component can be operated independently and therefore all three components can be
143 run simultaneously, allowing for multiple samples to be processed at the same time. The vacuum line

144 for removing meteoric ^{14}C currently accommodates up to six silica glass tubes; however, this number
145 can easily be increased. Likewise, the custom-built high-temperature tube furnace can accommodate
146 up to three fused silica glass tubes. The UHV extraction system allows the processing of two samples
147 per day, which is a substantial improvement over the current two days per sample that can be
148 achieved with other extraction scheme designs. Secondly, the use of fused silica glass tubes and a
149 tube furnace also means that there is more flexibility with the amount of quartz that can be
150 analysed. The current design can accommodate samples ranging between 0.5 to 4 grams of clean
151 quartz, however, larger samples could also be analysed by combining multiple fused silica tubes.

152

153 **3.2. Extraction blanks**

154 To estimate the magnitude of contaminant ^{14}C introduced during processing, we prepared a set of
155 full procedural blanks, using various amounts of synthetic quartz that should be free of any *in-situ*
156 ^{14}C . Further, experiments using synthetic quartz that has a similar matrix to a natural sample are
157 more representative than blank estimates using empty fused silica glass tubes. The synthetic quartz
158 used in our experiments was sourced from one single crystal that was crushed, sieved to 250 – 500
159 microns, and cleaned following procedures described in Kohl and Nishiizumi (1992). Synthetic quartz
160 analyses were done on both ANTARES at ANSTO and MICADAS at ETH Zürich, using between 0.5 to 3
161 grams of material, with two samples being direct splits: DQ48 / 80763.1.1, and DQ49 / 80763.2.1,
162 respectively (Fig. 2-A and Tables 1 and 2). Approximately 500 μg of CaCO_3 carrier (equivalent of 60 μg
163 C) were added to samples 80763.4.1, DQ48 / 80763.1.1, and DQ49 / 80763.2.1, whereas the rest of
164 synthetic quartz samples were processed with no carrier. Of the latter, those that were analysed on
165 ANTARES were diluted with dead CO_2 gas during graphitisation. Results average to $(0.98 \pm 0.68) \times 10^4$
166 atoms ($\pm 1\sigma$, $n=10$), with the samples graphitised and analysed on ANTARES yielding statistically
167 indistinguishable values from those analysed on MICADAS, namely $(1.01 \pm 0.77) \times 10^4$ atoms ($n=7$), as
168 compared to $(0.92 \pm 0.22) \times 10^4$ atoms ($n=3$), respectively. The larger spread in the ANTARES values
169 could be the result of the additional graphitisation step, however no firm interpretation can be made
170 due to the relatively low number of data points from MICADAS ($n=3$). Nevertheless, the $\sim 1 \times 10^4$
171 atoms *in-situ* ^{14}C full procedural blanks are consistent with those of Fülöp et al. (2015a). Unlike in the
172 case of Fülöp et al. (2015a), however, we do not observe a relationship between obtained *in-situ* ^{14}C
173 atoms and amount of synthetic quartz analysed. This could be due to the full Kohl and Nishiizumi
174 (1992) cleaning procedure applied to the crushed synthetic quartz material prior to analysis.

175

176 **3.3. Standard material**

177 *In-situ* ^{14}C results from samples CRONUS-R (CRR) and CRONUS-A (CRA) are shown in Fig. 2 (B and C)
178 and Tables 1 and 2, respectively. CRR and CRA are inter-comparison samples distributed as part of

179 the wider CRONUS-Earth and CRONUS-EU cosmogenic nuclide inter-comparison projects aimed at
180 assessing cosmogenic nuclide analysis accuracy and precision (Jull et al., 2015).

181

182 CRR is a beach sand collected from the Revere beach in Massachusetts USA (latitude: 42.43 °N,
183 longitude: 70.98 °W). Previous *in-situ* ¹⁴C analyses of CRR by Fülöp et al. (2015a) suggest that this is a
184 low-level sample. Our analyses yield a mean blank-corrected *in-situ* ¹⁴C concentration in CRR of $(2.58$
185 $\pm 1.12) \times 10^4$ atoms.g⁻¹ (n=11, $\pm 1\sigma$), however the mean value measured as graphite on ANTARES is
186 numerically larger but well within $\pm 1\sigma$ for the CRR measured as CO₂ on MICADAS (Fig. 2-B2): $(3.18 \pm$
187 $1.09) \times 10^4$ (n=6) and $1.87 \pm 0.69 \times 10^4$ atoms.g⁻¹ (n=5), respectively. Of the three samples where
188 direct splits were analysed on both accelerators, results overlap (to within $\pm 1\sigma$) in one sample (CX74
189 / 80787.4.1) and for the other two, results obtained from graphite are substantially higher than
190 those obtained from CO₂ gas (Fig. 2-B1). The latter suggests that with low-level samples such as CRR,
191 contributions from the graphitisation step to blank magnitude and variability may be important.

192

193 CRA was collected from an exposed sandstone outcrop from Antarctica (latitude: 77.88 °S, longitude:
194 160.94 °E, elevation: 1612 m a.s.l.) and has a consensus mean (n=23) *in-situ* ¹⁴C concentration of
195 $(6.93 \pm 0.44) \times 10^5$ atoms.g⁻¹ ($\pm 1\sigma$) based on mean values reported by four different AMS laboratories
196 ranging between $(6.51 \pm 0.33) \times 10^5$ to $(7.25 \pm 0.36) \times 10^5$ atoms.g⁻¹ (Jull et al., 2015). Our
197 measurements of CRA yield a mean of $(6.93 \pm 0.44) \times 10^5$ atoms.g⁻¹ *in-situ* ¹⁴C (n=14, $\pm 1\sigma$), a value
198 identical with that reported in Jull et al. (2015). Our measurements of CRA are also consistent with
199 the mean value reported in Fülöp et al. (2015a), namely $(6.72 \pm 0.71) \times 10^5$ atoms.g⁻¹ (Fig. 2-C).
200 Results obtained from graphite show mean values and spread indistinguishable from that for CO₂,
201 namely: $(6.74 \pm 0.70) \times 10^5$ atoms.g⁻¹ for graphite on ANTARES, and $(6.55 \pm 0.63) \times 10^5$ atoms.g⁻¹ for
202 CO₂ on MICADAS.

203

204 In addition to CRR and CRA, we also report results from CRONUS-N (CRN), the third inter-comparison
205 sample distributed as part of the CRONUS-Earth and CRONUS-EU cosmogenic nuclide inter-
206 comparison projects. CRN is a beach sand collected from Noosa beach in Queensland, Australia
207 (latitude: 26.40 °S, longitude: 153.12 °E). Similarly to CRR, CRN is also a low-level sample, with
208 previous analyses on MICADAS yielding a mean (n=5) *in-situ* ¹⁴C concentration of $(1.27 \pm 0.70) \times 10^4$
209 atoms.g⁻¹ (Lupker et al., 2015). Our analyses of four samples (two as graphite on ANTARES and two as
210 CO₂ gas on MICADAS) yield an average *in-situ* ¹⁴C concentration for CRN of $(3.26 \pm 1.59) \times 10^4$
211 atoms.g⁻¹ (Tables 1 and 2). This value, although higher, overlaps within uncertainty with that
212 reported in Lupker et al. (2015). Both Lupker et al.'s and the CRN results reported here exhibit a low
213 reproducibility (standard deviations of ~50%) that highlights the sensitivity of analyses in these low-
214 level samples to variability in system blanks. The low reproducibility of the CRN and CRR results may

215 also be due to impurities in these samples that are not efficiently removed during quartz purification,
216 or due to these standard materials not being homogeneous, the effect of both being amplified by the
217 low *in-situ* ¹⁴C concentration present.

218

219 **4. Summary**

220 The new ANSTO – UOW *in-situ* ¹⁴C extraction facility is now in routine operation. The design and
221 processing scheme follows the same setup developed at the University of Cologne. The modular
222 construction allows the three main processing stages to function independently allowing a relatively
223 rapid sample throughput – two samples per day – and can accommodate samples ranging between
224 0.5 to 4 grams of clean quartz. The extraction system yields low systems blanks ($\sim 1 \times 10^4$ atoms of *in-*
225 *situ* ¹⁴C) and demonstrates good reproducibility, measurements on the CRONUS-A inter-comparison
226 material yielding *in-situ* ¹⁴C concentrations that agree with those reported in the literature. The low
227 system blanks also permit the analysis of low-level samples such as CRONUS-R and CRONUS-N, albeit
228 with reduced reproducibility.

229

230 **Acknowledgements**

231 Financial support was provided by the University of Wollongong's Faculty of Science Medicine and
232 Health, the Centre for Archaeological Science (CAS), the GeoQuEST Research Centre, and the
233 National Collaborative Research Infrastructure Strategy (NCRIS). We also acknowledge assistance
234 from David Button, Krista Simon, Charles Mifsud, and support from Centre for Accelerator Science
235 staff at ANSTO.

236

237 **List of references**

238 Balco G., 2011, Contributions and unrealized potential contributions of cosmogenic-nuclide exposure
239 dating to glacier chronology, 1990–2010, **Quaternary Science Reviews**, Volume 30, Issues 1–2,
240 2011, Pages 3-27, DOI: 10.1016/j.quascirev.2010.11.003.

241 Brown R.M., Andrews H.R., Ball G.C., Burn N., Imahori Y., Milton J.C.D., Fireman E.L., 1984, ¹⁴C
242 content of ten meteorites measured by tandem accelerator mass spectrometry, **Earth and**
243 **Planetary Science Letters**, Volume 67, Issue 1, Pages 1-8, DOI: 10.1016/0012-821X(84)90033-5.

244 Cresswell R.G., Miura Y., Beukens R.P., Rucklidge J.C., 1983, ¹⁴C terrestrial ages of nine Antarctic
245 meteorites using CO and CO₂ temperature extractions, **Proceedings of the NIPR Symposium on**
246 **Antarctic Meteorites**, Volume 6, Pages 381-390.

247 Des Marais D.J., 1983, Light element geochemistry and spallogeneis in lunar rocks, **Geochimica et**
248 **Cosmochimica Acta**, Volume 47, Issue 10, Pages 1769-1781, DOI: 10.1016/0016-7037(83)90025-X.

249 Des Marais D.J., Moore J.G., 1984, Carbon and its isotopes in mid-oceanic basaltic glasses, **Earth and**
250 **Planetary Science Letters**, Volume 69, Issue 1, 1984, Pages 43-57, DOI: 10.1016/0012-
251 821X(84)90073-6.

252 Fahrni S.M., Wacker L., Synal H.-A., Szidat S., 2013, Improving a gas ion source for ¹⁴C AMS, **Nuclear**
253 **Instruments and Methods in Physics Research Section B: Beam Interactions with Materials and**
254 **Atoms**, Volume 294, Pages 320-327, DOI: 10.1016/j.nimb.2012.03.037.

255 Fink D., Hotchkis M., Hua Q., Jacobsen G., Smith A.M., Zoppi U., Child D., Mifsud C., van der Gaast H.,
256 Williams A., Williams M., 2004, The ANTARES AMS facility at ANSTO, **Nuclear Instruments and**
257 **Methods in Physics Research Section B: Beam Interactions with Materials and Atoms**, Volumes
258 223–224, Pages 109-115, DOI: 10.1016/j.nimb.2004.04.025.

259 Fülöp R.-H., Bishop P., Fabel D., Cook G.T., Everest J., Schnabel C., Codilean A.T., Xu S., 2015b,
260 Quantifying soil loss with in-situ cosmogenic ¹⁰Be and ¹⁴C depth-profiles, **Quaternary**
261 **Geochronology**, Volume 27, Pages 78-93, DOI: 10.1016/j.quageo.2015.01.003.

262 Fülöp R.-H., Naysmith P., Cook G.T., Fabel D., Xu S., Bishop, P., 2010, Update on the performance of
263 the SUERC in situ cosmogenic ¹⁴C extraction line, **Radiocarbon**, Volume 52, Pages 1288-1294. DOI:
264 10.1017/S0033822200046373.

265 Fülöp R.-H., Wacker L., Dunai T.J., 2015a, Progress report on a novel in situ ¹⁴C extraction scheme at
266 the University of Cologne, **Nuclear Instruments and Methods in Physics Research Section B:**
267 **Beam Interactions with Materials and Atoms**, Volume 361, Pages 20-24, DOI:
268 10.1016/j.nimb.2015.02.023.

269 Goehring B.M., Schimmelpfennig I., Schaefer J.M., 2014, Capabilities of the Lamont-Doherty earth
270 observatory in situ ¹⁴C extraction laboratory updated, **Quaternary Geochronology**, Volume 19,
271 Pages 194-197, DOI: 10.1016/j.quageo.2013.01.004.

272 Hippe K., Kober F., Baur H., Ruff M., Wacker L., Wieler R., 2009, The current performance of the in
273 situ ¹⁴C extraction line at ETH, **Quaternary Geochronology**, Volume 4, Pages 493-500, DOI:
274 10.1016/j.quageo.2009.06.001.

275 Hippe K., Kober F., Zeilinger G., Ivy-Ochs S., Maden C., Wacker L., Kubik P.W., Wieler R., 2012,
276 Quantifying denudation rates and sediment storage on the eastern Altiplano, Bolivia, using
277 cosmogenic ¹⁰Be, ²⁶Al, and in situ ¹⁴C. **Geomorphology**, Volume 179, Pages 58-70, DOI:
278 10.1016/j.geomorph.2012.07.031.

279 Hippe K., Lifton N.A., 2014, Calculating isotope ratios and nuclide concentrations for in situ
280 cosmogenic ¹⁴C analyses. **Radiocarbon**, Volume 56, Pages 1167-1174, DOI: 10.2458/56.17917.

281 Huang T.J., Tsai D.H., 2003, CO oxidation behavior of copper and copper oxides, **Catalysis Letters**,
282 Volume 87, Pages 173-178, DOI: 10.1023/A:1023495223738.

283 Jull A.J.T., Donahue D.J., Linick T.W., 1989, Carbon-14 activities in recently fallen meteorites and
284 Antarctic meteorites, **Geochimica et Cosmochimica Acta**, Volume 53, Issue 8, Pages 2095-2100,
285 DOI: 10.1016/0016-7037(89)90327-X.

286 Jull A.J.T., Scott E.M., Bierman P., 2015, The CRONUS-Earth inter-comparison for cosmogenic isotope
287 analysis, **Quaternary Geochronology**, Volume 26, Pages 3-10, DOI: 10.1016/j.quageo.2013.09.003.

288 Kober F., Hippe K., Salcher B., Ivy-Ochs S., Kubik P.W., Wacker L., Hahnen N., 2012, Debris-flow-
289 dependent variation of cosmogenically derived catchment-wide denudation rates, **Geology**,
290 Volume 40, Pages 935-938, DOI: 10.1130/G33406.1.

291 Kohl C.P., Nishiizumi K., 1992, Chemical isolation of quartz for measurement of in-situ-produced
292 cosmogenic nuclides, **Geochimica et Cosmochimica Acta**, Volume 56, Issue 9, 1992, Pages 3583-
293 3587, DOI: 10.1016/0016-7037(92)90401-4.

294 Lifton N.A., Jull A.J.T., Quade J., 2001, A new extraction technique and production rate estimate for in
295 situ cosmogenic ¹⁴C in quartz, **Geochimica et Cosmochimica Acta**, Volume 65, Issue 12, Pages
296 1953-1969, DOI: 10.1016/S0016-7037(01)00566-X.

297 Lupker M., Hippe K., Wacker L., Kober F., Maden C., Braucher R., Bourlès D., Vidal Romani J.R., Wieler
298 R., 2015, Depth-dependence of the production rate of in situ ¹⁴C in quartz from the Leymon High
299 core, Spain, **Quaternary Geochronology**, Volume 28, Pages 80-87, DOI:
300 10.1016/j.quageo.2015.04.004.

301 Pineau F., Javoy M., 1994, Strong degassing at ridge crests: The behaviour of dissolved carbon and
302 water in basalt glasses at 14°N, Mid-Atlantic Ridge, **Earth and Planetary Science Letters**, Volume
303 123, Issues 1–3, Pages 179-198, DOI: 10.1016/0012-821X(94)90266-6.

304 Smith A.M., Yang B., Hua Q., Mann M., 2010, Laser-heated microfurnace - gas analysis and graphite
305 morphology, **Radiocarbon**, Volume 52, Issues 2-3, Pages 768-782, DOI:
306 10.1017/S0033822200045781.

307 Smith A.M., Hua Q., Williams A., Levchenko, V., Yang B., 2010, Developments in micro-sample ¹⁴C
308 AMS at the ANTARES AMS facility, **Nuclear Instruments and Methods in Physics Research Section**
309 **B: Beam Interactions with Materials and Atoms**, Volume 268, Pages 919-923, DOI:
310 10.1016/j.nimb.2009.10.064

311 Watson E.B., Sneeringer M.A., Ross A., 1982, Diffusion of dissolved carbonate in magmas:
312 Experimental results and applications, **Earth and Planetary Science Letters**, Volume 61, Issue 2,
313 Pages 346-358, DOI: 10.1016/0012-821X(82)90065-6.

314 Yang B., Smith A.M., Long S., 2015, Second generation laser-heated microfurnace for the preparation
315 of microgram-sized graphite samples, **Nuclear Instruments and Methods in Physics Research**
316 **Section B: Beam Interactions with Materials and Atoms**, Volume 361, Pages 363-371, DOI:
317 10.1016/j.nimb.2015.02.009.

318

319 **Figure Captions**

320 Figure 1: Diagram describing the ANSTO / University of Wollongong *in-situ* ¹⁴C extraction scheme. See
321 text for more details.

322

323 Figure 2: *In-situ* ¹⁴C measurement results for (A) synthetic quartz material, (B) the CRONUS-R and (C)
324 CRONUS-A inter-comparison materials. Red symbols are used for samples analysed as graphite on
325 ANTARES (ANSTO) and blue symbols for samples analysed as CO₂ gas on MICADAS (ETH Zürich). Grey
326 arrows indicate split samples. Solid and dotted lines in (A1) and (B1) represent mean *in-situ* ¹⁴C
327 concentrations obtained on ANTARES and MICADAS respectively. Grey band in (C1) represents one
328 standard deviation of the mean *in-situ* ¹⁴C concentration (solid line) obtained for the CRONUS-A
329 material by this study. Dashed line in (C1) represents mean CRONUS-A *in-situ* ¹⁴C concentration
330 reported in Jull et al. (2015). Box plots in (C2) are based on data reported in Fülöp et al. (2015) and
331 Jull et al. (2015) – labs A to C.

332

333 **Table Captions**

334 Table 1: Summary of *in-situ* ¹⁴C analyses on graphite targets done on ANTARES at ANSTO.

335 Table 2: Summary of *in-situ* ¹⁴C analyses on CO₂ gas done on MICADAS at ETH-Zürich.

336

337 Table 1.

AMS #	$^{14}\text{C}/^{12}\text{C}^a$ $\times 10^{-15}$	$\pm [^{14}\text{C}/^{12}\text{C}]^a$ $\times 10^{-15}$	$\delta^{13}\text{C}^b$ ‰	$\pm [\delta^{13}\text{C}]^b$	VS ^c	N14 ^d [atoms]	$\pm [\text{N14}]^d$ [atoms]	DCO ₂ ^e [atoms]	$\pm [\text{DCO}_2]^e$ [atoms]	corr. N14 ^f [atoms]	$\pm [\text{corr. N14}]^f$ [atoms]	Qtz Mass ^g [g]	$\pm [\text{Qtz Mass}]^g$ [g]	$^{14}\text{C conc.}^h$ [at.g ⁻¹]	$\pm [^{14}\text{C conc.}]^h$ [at.g ⁻¹]
System blanks (synthetic quartz)															
CX61	9.84	1.52	-7.00	-0.07	0.0419	10454	1633					0.53157	0.00005		
DQ48	4.10	0.47	-6.33	-0.06	0.1164	11966	1394					2.02186	0.00005		
DQ49	7.26	0.82	-5.42	-0.05	0.1418	26248	2935					3.00465	0.00005		
DQ52	15.58	1.52	-7.00	-0.07	0.0118	4674	477					2.01428	0.00005		
DQ53	17.45	2.34	-7.00	-0.07	0.0124	5480	740					2.01487	0.00005		
DQ54	11.83	1.29	-7.00	-0.07	0.0123	3707	400					3.03954	0.00005		
DQ55	27.65	2.34	-7.00	-0.07	0.0120	8424	729					3.00747	0.00005		
Cronus-R (CRR)															
CX74	18.74	1.29	-25.51	-0.26	0.0892	40916	2919			30780	8266	1.01123	0.00005	30438	8174
DL99	14.41	0.94	-30.72	-0.31	0.2546	88680	5647			78543	9576	3.01776	0.00005	26027	3173
DM08	22.26	1.41	-30.72	-0.31	0.1035	55758	3609			45622	8534	1.03075	0.00005	44261	8279
DQ42	11.48	0.82	-28.83	-0.29	0.0930	25878	1943			15741	7973	1.01527	0.00005	15505	7853
DQ90	21.20	1.76	-27.57	-0.28	0.1888	97627	8275			87490	11326	2.01420	0.00005	43437	5623
DQ91	15.35	0.82	-40.97	-0.41	0.2859	104197	5352			94061	9404	3.03038	0.00005	31039	3103
Cronus-A (CRA)															
CX68	921.59	11.60	-4.67	-0.05	0.0266	624707	10800	5481	2	609090	13283	1.02207	0.00005	595937	12996
CX71	171.50	2.58	-4.67	-0.05	0.1808	790581	14064	57157	43	723288	16050	1.02416	0.00005	706226	15671
DM02	3156.87	38.89	-3.52	-0.04	0.0300	2416668	40728			2406532	41456	3.00835	0.00005	799951	13780
DM03	3066.90	30.11	-6.95	-0.07	0.0287	2235314	33980			2225178	34849	3.00333	0.00005	740904	11604
DM04	3143.28	63.38	-6.13	-0.06	0.0174	1386464	34003			1376328	34871	2.06708	0.00005	665832	16870
DM05	3287.49	468.12	-2.07	-0.02	0.0177	1490349	213192			1480213	213332	2.06214	0.00005	717804	103452
DM06	3520.96	100.16	-4.67	-0.05	0.0069	616701	24026			606565	25239	1.03129	0.00005	588161	24474
DQ57	2944.48	69.35	-4.67	-0.05	0.0083	625640	20448			615504	21861	1.00422	0.00005	612917	21769
DQ92	3380.50	34.79	-4.67	-0.05	0.0146	1261851	23281			1251715	24531	2.03449	0.00005	615248	12058
DQ93	3078.03	33.86	-4.67	-0.05	0.0181	1423547	24994			1413410	26163	2.03922	0.00005	693113	12830
Cronus-N (CRN)															
CX67	124.76	5.74	-13.84	-0.14	0.0389	121600	5746	5926	2	105538	9634	2.02265	0.00005	52178	4763
DB94	72.28	3.51	-13.84	-0.14	0.0460	83193	4143	7947	3	65110	8773	2.02157	0.00005	32207	4340

a) Measured $^{14}\text{C}/^{12}\text{C}$ ratio and uncertainty ($\pm 1\sigma$)

339 Table 2.

AMS #	$^{14}\text{C}/^{12}\text{C}$ ^a	$\pm [^{14}\text{C}/^{12}\text{C}]$ ^a	$\delta^{13}\text{C}$ ^b	$\pm [\delta^{13}\text{C}]$ ^b	VS ^c	N14 ^d	$\pm [\text{N14}]$ ^d	DCO ₂ ^e	$\pm [\text{DCO}_2]$ ^e	corr. N14 ^f	$\pm [\text{corr. N14}]$ ^f	Qtz Mass ^g	$\pm [\text{Qtz Mass}]$ ^g	^{14}C conc. ^h	$\pm [^{14}\text{C} \text{ conc.}]$ ^h
	$\times 10^{-15}$	$\times 10^{-15}$	‰			[atoms]	[atoms]	[atoms]	[atoms]	[atoms]	[atoms]	[g]	[g]	[at.g ⁻¹]	[at.g ⁻¹]
System blanks (synthetic quartz)															
80763.1.1	3.09	0.54	-6.33	-0.06	0.1164	8669	1520					2.02186	0.00005		
80763.2.1	2.13	0.49	-5.42	-0.05	0.1418	7306	1676					3.00465	0.00005		
80763.4.1	5.52	0.64	-9.24	-0.09	0.0868	11572	1347					2.00757	0.00005		
Cronus-R (CRR)															
80787.1.1	8.30	0.66	-27.57	-0.28	0.1888	37837	3029			28654	3731	2.01420	0.00005	14226	1852
80787.2.1	9.59	0.69	-40.97	-0.41	0.2859	66196	4788			57014	5260	3.03038	0.00005	18814	1736
80787.3.1	8.94	0.92	-28.83	-0.29	0.0930	20073	2067			10890	3003	1.01527	0.00005	10726	2958
80787.4.1	17.79	1.14	-25.51	-0.26	0.0892	38343	2477			29160	3299	1.01123	0.00005	28837	3262
80787.5.1	13.32	0.91	-38.22	-0.38	0.1588	51083	3508			41900	4130	2.01025	0.00005	20843	2054
Cronus-A (CRA)															
80789.1.1	2988.56	22.64	-6.13	-0.06	0.0174	1252146	19912			1242964	20031	2.06708	0.00005	601314	9690
80789.2.1	2991.35	37.15	-2.07	-0.02	0.0177	1277669	23770			1268487	23870	2.06214	0.00005	615131	11575
80789.3.1	3095.21	85.14	-3.52	-0.04	0.0300	2238937	66742			2229755	66778	3.00835	0.00005	741189	22197
80789.4.1	2888.66	32.30	-6.95	-0.07	0.0287	2003192	32292			1994009	32365	3.00333	0.00005	663933	10776
Cronus-N (CRN)															
81185.2.1	28.24	1.31	-13.42	-0.13	0.1382	94289	4490	17332	37	67775	4991	2.06792	0.00005	32775	2414
81185.3.1	64.74	3.88	-14.27	-0.14	0.0321	50180	3059	14645	31	26352	3756	2.00482	0.00005	13144	1873

a) Measured $^{14}\text{C}/^{12}\text{C}$ ratio and uncertainty ($\pm 1\sigma$)

b) $\delta^{13}\text{C}$ value of the analyzed CO₂ gas

c) Total volume of the extracted and dead CO₂ gas at STP

d) Number of ^{14}C atoms and uncertainty ($\pm 1\sigma$) in the measured sample

e) Number of ^{14}C atoms and uncertainty ($\pm 1\sigma$) introduced by the "dead" CO₂ dilution

f) Number of ^{14}C atoms of the sample (and uncertainty $\pm 1\sigma$) corrected for the addition of "dead" CO₂ and corrected for a blank of $1.01 \pm 0.77 \times 10^4$ atoms ^{14}C

g) Mass of quartz analysed and uncertainty ($\pm 1\sigma$)

h) ^{14}C concentration of the sample (atoms.gram⁻¹) and associated uncertainty ($\pm 1\sigma$)

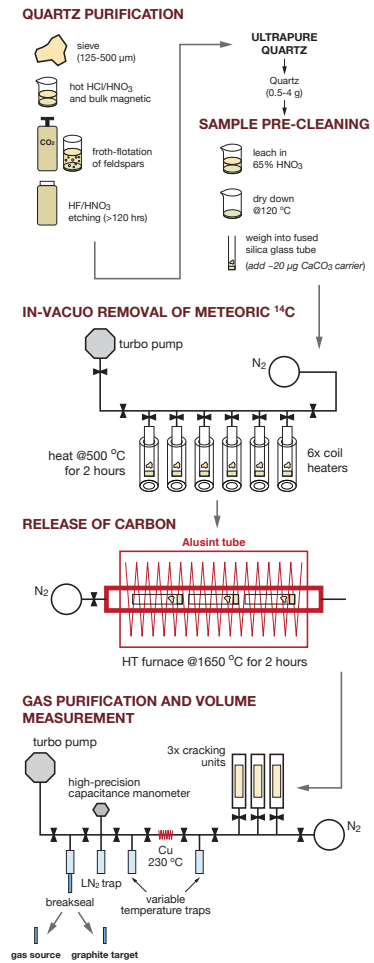


Figure 1.

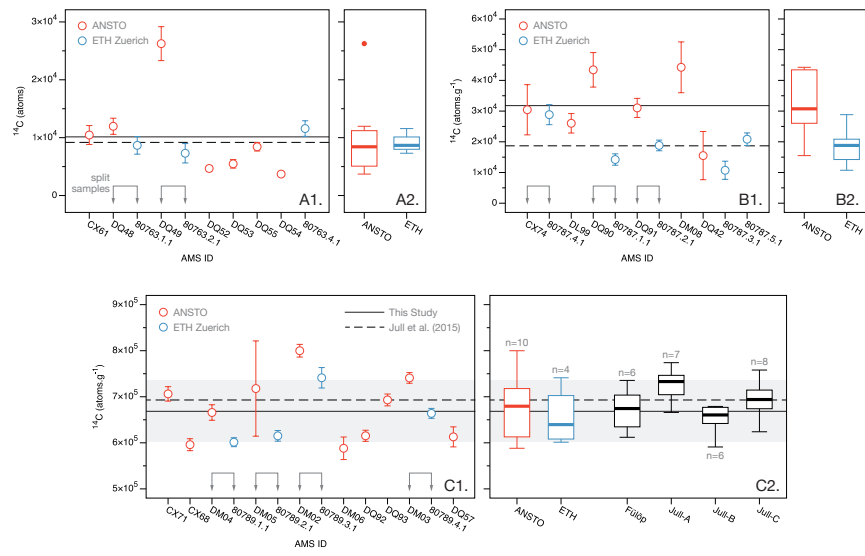


Figure 2.